Contributed Papers from Materials Science and Technology 2016 (MS&T16)
October 23 – 27, 2016, Salt Palace Convention Center, Salt Lake City, Utah USA

COMPARISON OF CONVENTIONAL OPEN-CELL ALUMINUM FOAM AND ITS ADDITIVELY MANUFACTURED TWIN

Kristoffer Matheson, Kory Cross, Iman Javahery, Jayden Plumb, Ashley Spear

Department of Mechanical Engineering, University of Utah, Salt Lake City, UT, USA

Keywords: metallic foam, 6061, powder bed fusion, DMLS, 3D printing, tomography

Abstract

With the exciting potential of additive manufacturing of metals to produce geometrically complex structures come many unknowns and uncertainties regarding the process-microstructure-property relationships of the additively manufactured (AM) parts, especially in comparison to their conventionally manufactured counterparts. This work attempts to elucidate some key differences between AM and cast parts by comparing the deformation response of two sub-components that are nearly identical (deemed, "twins") except for the route by which each was manufactured. The sub-components are open-cell foams of aluminum alloy 6061. The baseline open-cell foam is conventionally produced via investment casting. Two copies are produced using laser powder bed fusion. An in-situ load frame is developed to measure the full-field deformation of the foams under compressive loading using X-ray micro-computed tomography. Differences among the aluminum foams are exemplified by the load-displacement response and by local deformation of isolated ligaments within the volume. This proof-of-concept study investigates a structural geometry that exposes both the advantages and potential disadvantages of additive manufacturing in comparison to traditional manufacturing routes.

Introduction

Open-cell metallic foams are an exciting class of structural-material systems that comprise a network of interconnected metallic ligaments, resulting in an interesting structural hierarchy [1]—namely, the component scale of the structure, the topological scale of the foam, and the grain scale of individual ligaments. These low-density, hierarchical materials have garnered much attention over the past two decades based on their recognized potential for use in multi-functional applications [2]. For example, in addition to serving as light-weight, load-bearing, structures, open-cell metallic foams have the potential to serve concurrently as electrodes for energy-storage devices, as hosts for newly generated bone and blood vessels in biomedical implants, or as impact absorbers and noise insulators for advanced high-speed ground transportation. In this way, the foams may simultaneously act as structures and devices, thereby increasing dramatically the efficiency of entire systems.

The conventional route by which open-cell metallic foams are produced is investment casting [3,4], whereby a pre-existing polymer material is "invested" to produce a final product with the same geometry as the invested shape. A negative mold is needed in the investment casting process in order to produce a final product with the same geometry as the original invested shape. Commonly, a ceramic slurry (e.g. silica (SiO_2), calcium sulfate ($CaSO_4$), and water) is used to create the mold [5]. The ceramic mold is created by introducing the ceramic slurry into a reticulated polyurethane foam and allowing the slurry to harden. Upon hardening, the material must be heated gradually in a stepwise manner in order to prevent the mold from cracking. The

polymer foam begins to burn out around 240° C, and will be completely evaporated by the end of the ceramic baking process [5]. Once the polymer has completely evaporated, the hardened ceramic mold remains in the negative shape of the original polymer foam. The molten metal is then cast using the ceramic mold. Once the metal has solidified, the mold is removed, generally through a simple leaching process. Leaching is a process whereby a liquid acid is used to dissolve the mold and separate it from the solidified aluminum without damaging the surface of the aluminum.

A possible alternative to investment casting is additive manufacturing by, for example, laser powder bed fusion (LPBF). LPBF is a process that utilizes a 3D CAD model to produce a metallic volume that has a reported material density of approximately 100% [6]. There are four steps in the LPBF process: 3D-CAD model slicing, metallic powder deposition, laser scanning, and lowering of the bed platform. The first step involves creating and slicing a 3D CAD model into layers to be read by the LPBF machine. A thin layer of metallic powder is then deposited onto the substrate and a laser is used to scan across and melt the desired regions of powder. After scanning is completed on the given layer, the platform is lowered and a new layer of powder is deposited onto the existing layer. This process is repeated until all of the layers of the 3D CAD model have been scanned and solidified. Upon completion, the solid geometry is removed from the powder bed.

Open-cell metallic foams are selected as the structure of interest in this proof-of-concept study due to the complex geometry of the foam, which exposes both the potential advantages as well as disadvantages of metal additive manufacturing. For example, potential advantages of using additive manufacturing include the ability to produce such a complex geometry using less material and fewer processing steps. However, the complex geometry also precludes the ability to mechanically polish the surface after deposition, thereby exposing a potential disadvantage of as-deposited AM parts (viz., the increased surface roughness compared to conventional manufacturing routes).

The objective of the proof-of-concept study described in this paper is to compare the full-field deformation between conventional open-cell Al foam and copies produced using LPBF. A methodology is presented for creating "twins" of the foam by using a powder of the same metallic alloy and by using X-ray micro-computed tomography (micro-CT) to produce the required CAD file for additive manufacturing. Here, the word "twin" is connoted to mean that both the geometry and the alloy are intended to be identical, although the underlying microstructure is surely not. A common alloy between the commercially available open-cell foam and the commercially available powders for use in additive manufacturing is identified to be aluminum alloy 6061. Preliminary results are presented in terms of both local and global deformation of the open-cell Al foams.

Methods

Materials and Sample Preparation

The conventional method by which the open-cell foams are produced is investment casting, which is considered to be the baseline manufacturing method in this study. The investment-cast Al foam used in this study has a base alloy of 6061 (subjected to a T6 post-process heat treatment), and the nominal geometry of the foam has five pores per inch (5 ppi) and 10.5%

density. Two AM twins of the foam are created to replicate both the geometry and alloy of the baseline foam by using LPBF, specifically direct metal laser sintering.

As a proof-of-concept, two cylindrical samples are bored out of the bulk investment-cast foam using electrical discharge machining. One sample (10.2 mm diameter, 5.7 mm length) is used for characterization and comparison of grain structure, and the other (10.2 mm diameter, 18.3 mm length) is used for in-situ characterization and comparison of the crushing response. After machining, the cylindrical samples are imaged using a Varian BIR 150/130 micro-CT imaging system (15 μm voxel resolution). For each cylindrical sample of Al foam, the corresponding stack of tomograms is segmented and reconstructed in Avizo® to generate an STL file of the full volume.

The STL files are then used to create an approximate "twin" of each cylindrical sample of foam using LPBF. To ensure a valid comparison between foams, care was taken to obtain the same powder alloy as the alloy used in the commercially available investment-cast foam. The powder alloy is produced by Valimet, Inc., and has a special designation of AM 6061, which is reported to have spherical particles with average diameter of 34.2 μm [7]. The chemical composition for the 6061 alloy is provided in Table I.

Table I. Chemical composition of 6061 powder provided by Valimet, Inc. (% wt) [7]

Al	Mg	Si	Cu	Fe	Cr	Mn	Ti	Zn
Bal.	0.86	0.59	0.24	0.18	0.07	0.02	0.01	<0.01

The AM foam samples are produced using a Concept Laser M-Lab R LPBF system. The default (and proprietary) processing parameters for CL 31Al [8], which is Concept Laser's aluminum powder, are used. It is noted that no attempts are made in this proof-of-concept study to optimize the process parameters. One copy of the smaller sample and two copies of the larger sample are produced. Following the LPBF process, all of the samples are subjected to the default heat treatment specified in Concept Laser's datasheet for stress relieving aluminum [8]. The samples are heated up in one hour to 240°C and then maintained at temperature for six hours. The samples are then allowed to cool down in oven to 100°C. Finally, the samples are allowed to cool down in ambient atmosphere.

Microstructure Characterization

To enable a microstructure characterization and comparison, the foams must be carefully prepared and polished without damaging the individual ligaments. To accomplish this, each Al foam sample is set in a poly(methyl methacrylate) resin, otherwise known as acrylic. The acrylic resin protects the foam ligaments or struts from deforming during polishing. A quickset acrylic powder and liquid solution is used. The excess acrylic resin is sanded away and shaped using 180 grit (80 μm) silicon carbide paper. Each sample is then polished to a 0.05 μm RMS roughness rating through a series of polishing steps using an Allied Techprep 10-1000 mechanical polisher. Each sample is polished gradually using a series of polishing papers while ensuring the scratches from the previous paper are completely removed before moving on to the next paper. The first set of polishing paper used is silicon carbide and the order of polishing is 180 grit (80 μm), 320 grit (35 μm), 600 grit (15 μm). Diamond lapping film is then used with an order of 12 μm, 9 μm, 3 μm. Finally alumina suspension is used with an order of 1 μm, 0.3 μm, 0.05 μm. Upon completing mechanical polishing, a Fischione Model 1060 SEM Mill provided the final polish.

In-Situ Mechanical Testing

To monitor the full-field deformation of the Al foam during crushing, a specialized in-situ load frame was recently developed by the authors to enable collection of X-ray micro-CT data incrementally during mechanical loading. The load frame is compatible with the Varian BIR 150/130 X-ray micro-CT imaging system, has a low attenuation of X-rays, provides a 360° view of the sample while in the load frame, and maintains clean wire management that prevents any wires from obstructing the X-rays during scanning. Figure 1 shows a schematic of the load-frame design. A captive linear stepper motor applies force (or displacement) to the lower stage of the load frame. A rigid polycarbonate tube holds the upper mount in place and prevents upward displacement of the sample as force (displacement) is applied. The specimen is held in place by two transparent polycarbonate caps, which maintain axially symmetric load and keep the foam centered about the vertical axis to facilitate tracking the field of view. Figure 2 shows the actual load frame inside of the micro-CT chamber.

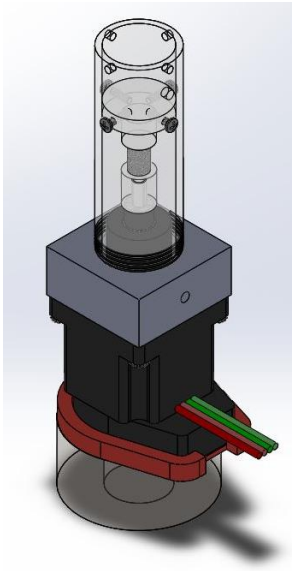

Figure 1. Schematic of in-situ load frame.

The 18.3 mm-long foam samples (one investment cast and two produced by LPBF) are loaded in displacement control to a total displacement of at least 12 mm (approximately 66% of initial length). Micro-CT scan images are collected every 2 mm of displacement while the displacement is held constant.

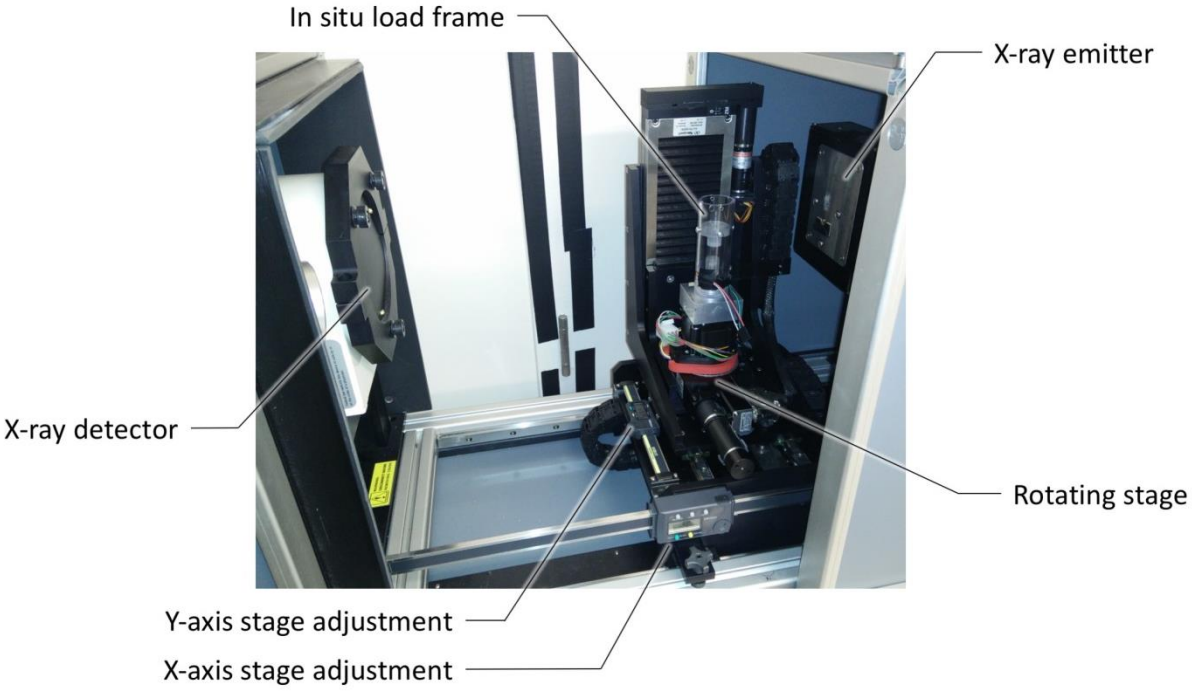

Figure 2. Load frame place inside the chamber of the Varian micro-CT scanner.

Results and Discussion

The applied load versus displacement response of the conventional (investment-cast) foam and the two LPBF twins is shown in Fig. 3. Each of the foams exhibits three general responses in the global force-displacement behavior: elastic response, followed by softening, followed by hardening. The apparent softening region is likely caused by localized yielding and buckling of individual ligaments. As the material densifies and the ligaments begin contacting one another, the foam regains load-carrying capacity and exhibits the apparent hardening behavior, represented by the average increase in load-displacement response. Each rise or drop along the curve is suspected to correspond to new surface contact or local ligament collapse, respectively. It is noted that because there are relatively few ligaments throughout the entire volume of foam, the load-displacement response of the aggregate appears to be especially sensitive to localized phenomena. It is expected that if the volume contained more ligaments (thus converging to a representative volume element, or RVE), the overall response would exhibit the same three regions of behavior but with less sensitivity to localized deformation.

The initial stiffness of the foam (slope of the elastic region) is similar for the two LPBF foams, but is slightly higher for the investment-cast foam. This could be due to the slight differences in the post-process heat treatments applied for the investment-cast and LPBF foams. Perhaps the more interesting discrepancies in behavior occur after elastic response, where the load-displacement varies dramatically among all three samples. For example, the investment-cast foam exhibits a more pronounced softening effect compared to the two LPBF foams. The authors suspect that this could be due to an overall more ductile behavior of the base material compared to the LPBF foam, which could have more of a brittle base material. While the authors do not have sufficient data to compare sample-to-sample variation for the investment-cast foam, it is apparent that there is significant variation between the two LPBF foams. The results suggest that there is an inherent variability that occurs due to the LPBF process. However, the observed variability could also be due to the volume of foam being below the limits of an RVE, as stated above. This remains the topic of ongoing study by the authors. Nonetheless, it is an interesting result that despite undergoing the exact same processing route with the same alloy and post-process heat treatment, the two LPBF foams exhibit a dramatically different load-displacement response.

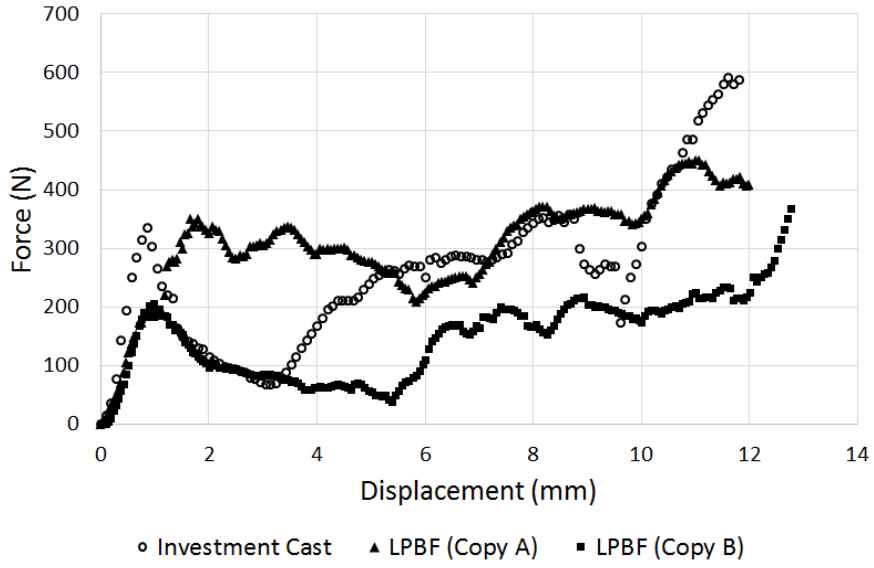

Figure 3. Load versus displacement of conventional open-cell Al 6061 foam and two copies produced by laser powder bed fusion.

Figure 4 depicts the 3D reconstructions of the Al foam samples from X-ray micro-CT captured at discrete values of applied displacement. The reconstructions are depicted from the same frame of reference to enable visual comparison. A visual assessment reveals that the globally deformed shape is slightly different for all three samples. A more localized comparison is shown for demonstration in Fig. 5. In the figure, an isolated region is shown at different stages throughout applied displacement, again captured from the same frame of reference among the three samples. The same ligament is circled for the three foams to point out the variability in both shape and amount of localized deformation of individual ligaments, which ultimately leads to the macroscopic variability shown in the load-displacement response in Fig. 3.

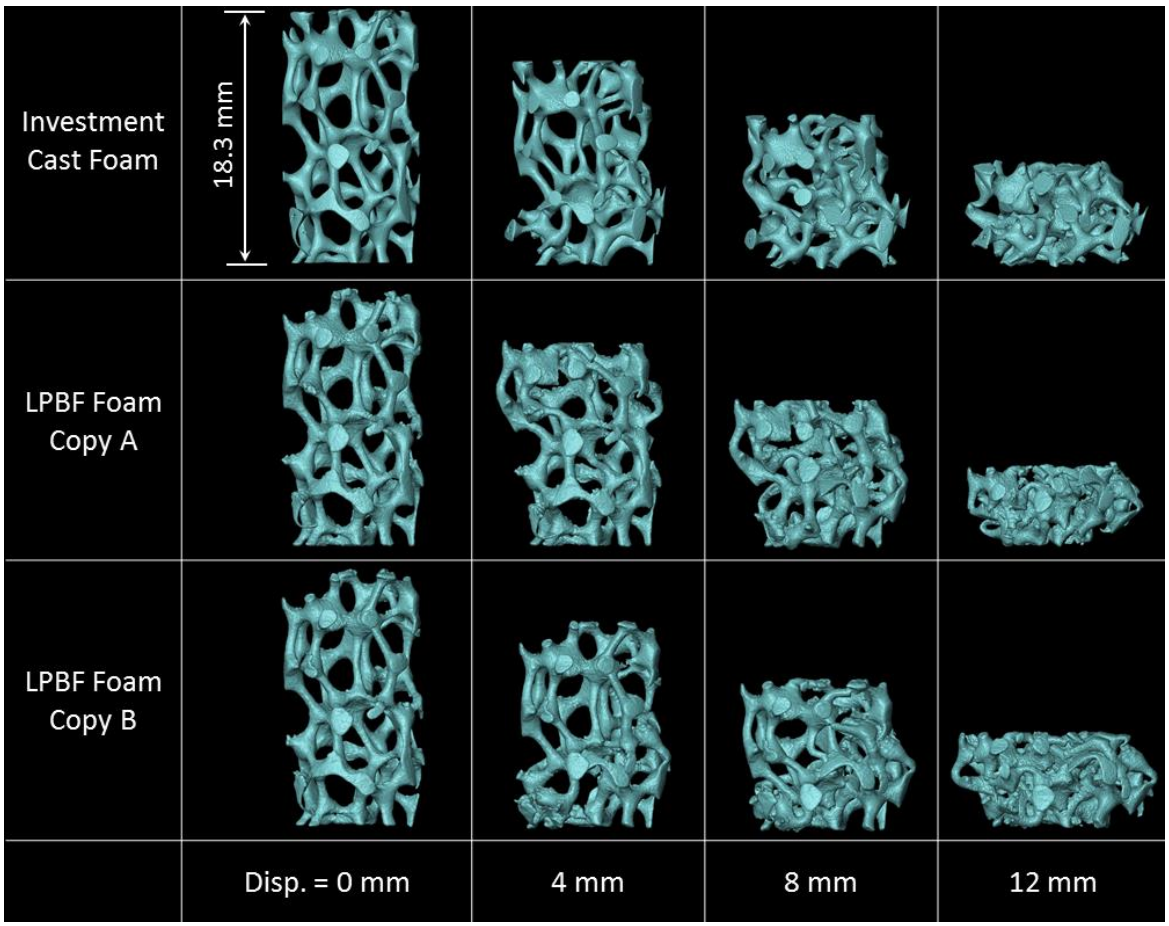

Figure 4. Deformed response of the investment-cast foam and two copies produced by laser powder bed fusion, depicted at the applied displacement levels indicated.

Optical micrographs are shown in Fig. 6 for a polished cross section of the investment-cast Al foam and the same cross section from the twin foam produced by LPBF. Inset figures show the same ligament cross section under higher (but equivalent) magnification. The inset micrographs show that the shape of the baseline ligament is not precisely replicated in the LPBF foam. There are two likely reasons for this. Perhaps the more obvious reason is that the additive manufacturing process has limited resolution with which it can physically represent the input CAD representation. A less obvious reason for the discrepancy could be due to the triangulated surface representation of the original geometry, viz., the size of the triangles that are used to

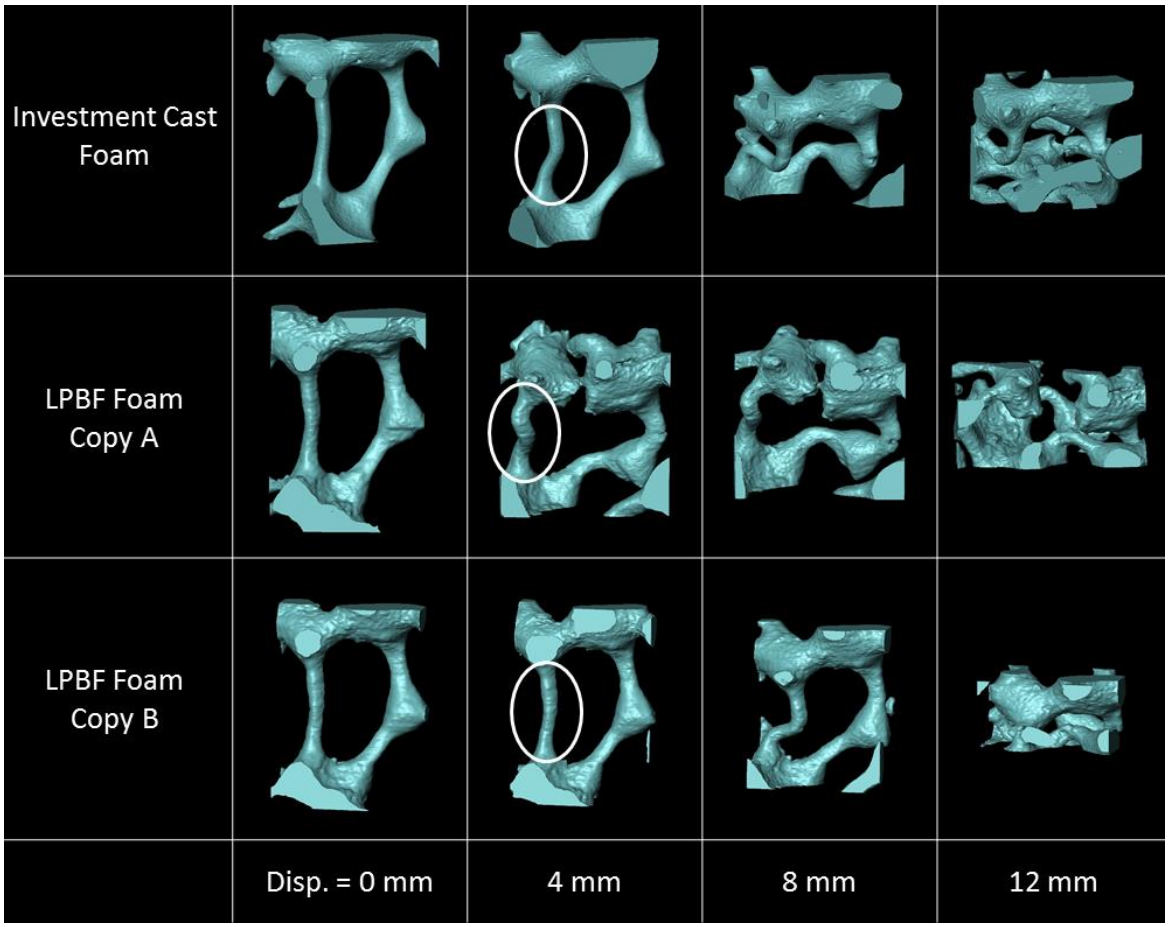

Figure 5. An isolated region from Fig. 4 shown in the same frame of reference among the three foam samples at the applied displacement levels indicated.

represent the surface in the STL file. However, the authors suspect that that latter explanation contributes less to the discrepancy than the former explanation. Finally, the contrast in the optical micrograph of the investment-cast foam reveals the underlying grain structure, where the grains appear to have dimensions on the order of 100 μm. The optical micrograph of the LPBF foam does not provide information about the underlying grain structure, though it is anticipated to be quite different than the original foam. Ongoing work by the authors is investigating the effect of grain structure on the overall difference in observed deformation of the foams.

Conclusions

A comparison is carried out between conventional open-cell foam of Al 6061 and "twins" produced via laser powder bed fusion. The duplicates, or twins, are produced using Al 6061 powder and X-ray tomography (micro-CT) data from the conventional foam. The full-field 3D response of the foams is characterized by collecting X-ray micro-CT data incrementally as the foams are crushed. Significant variability is observed among the global load-displacement responses of the foams, which is attributed to differences in the localized deformation among individual ligaments. The results motivate future work to investigate grain-scale effects.

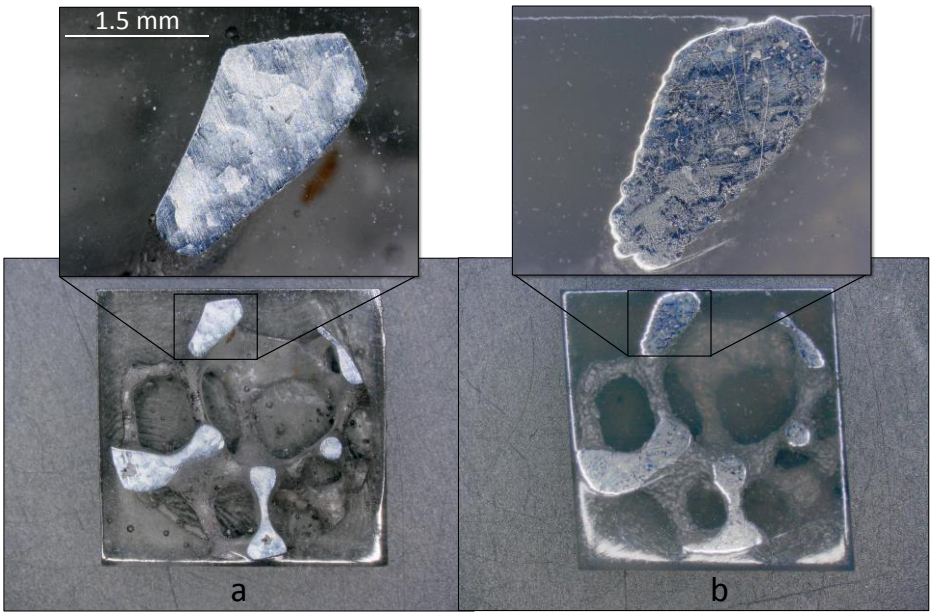

Figure 6. Polished cross sections of (a) the investment-cast Al 6061 foam and (b) its "twin" produced by laser powder bed fusion.

Acknowledgements

Gratitude is expressed to Dr. Michael Czabaj of the Utah Composites Laboratory for providing in-kind use of the Varian micro-CT system. This work is supported by the University of Utah Undergraduate Research Opportunities Program (UROP).

References

1. L. J. Gibson and M. F. Ashby (1999). Cellular Solids: Structure and Properties. Cambridge University Press.

2. A. G. Evans, J. Hutchinson, and M. Ashby (1998). Multifunctionality of cellular metal systems. *Progress in Materials Science*, 43(3):171–221.

3. H. N. Wadley (2002). Cellular metals manufacturing. *Advanced Engineering Materials*, 4(10):726–733.

4. M. F. Ashby, A. Evans, N.A. Fleck, L.J. Gibson, J.W. Hutchinson, H.N.G. Wadley (2000). Metal Foams: A Design Guide. Elsevier.

5. L. Wang, H. Li, F. Wang, and J. Ren (2005). Preparation of open-cell metal foams by investment cast. *China Foundry*, 2(1), 56-59.

6. S. Bremen, W. Meiners, A. Diatlov (2012). Selective Laser Melting a Manufacturing Technology for the Future? *Laser Technik Journal*, 2. DOI: 10.1002/latj.201290018

7. Larry Elam, Jr., Valimet, Inc., inspection certificate (private communication), 04 May 2016.

8. Concept Laser, material data sheet for CL 30AL/CL 31AL. http://www.conceptlaserinc.com/wp-content/uploads/2014/10/CL-AL30_31AL_Englisch.pdf